contact region extension [v_1] is measured through multiplying the number of voxels that is included in this extension by a voxel volume. This process is repeated iteratively and "a_i" and "v_i" are measured where i = 2, 3, 4, etc. This iteration is automatically stopped when at least one of the following conditions is satisfied in the same priority mentioned here: (1) when $a_i < 50$ mm^3, (2) when $v_i < 300$ mm^3, and (3) when $a_i \geq a_{i-1}$ and $a_{i-1} > 0$ (a local minimum of a_i is detected). The value "300 mm^3" was chosen experimentally to stop iteration before leakage into neighboring organs.

Other contact regions are re-extended in the same manner and added to the core region extension result. The results of one contact region and the core region extensions are illustrated [Fig. 11(f)].

2.C.4. Step 4: Refining the segmented liver

Refining the segmented liver is performed in two steps: (1) refining main BVs using a solid angle and (2) filling holes in 3D.

2.C.4.a. Refining main BVs using a solid angle. During classification of BVs of different organs (Sec. 2.B.2), some parts of main BVs are misclassified at the liver entrance, causing under- or oversegmentation. These BVs are refined as follows:

Each voxel of the segmented liver is checked with its 26 neighbors. When one or more of these neighbors is not a liver, this voxel is considered as a liver surface candidate. When these neighbors are included in main BVs, they are considered as intersecting voxels of liver with main BVs. Starting from each voxel of this intersection (X, Y, Z) as a center, a rectangular box of length 30 mm, width 30 mm, and height 30 mm is selected. Main BVs within this region are selected for classification using a solid angle [Fig. 12(a)]. A solid angle with a vertex at a voxel p of main BVs is defined as follows:[57]

A solid angle = Count 2/Count 1,

where "Count 1" represents the total number of vectors that are generated with equivalent angles from p to all voxels of the surface of a sphere centered at this voxel. "Count 2" represents the number of vectors that pass through the same sphere and intersect the segmented liver surface. The maximum checking region for intersection of these vectors with liver tissue is set to the surface of a sphere centered at p with a radius $r = 15$ mm. This radius is chosen experimentally to exclude the region of the liver surface marked with arrows [Fig. 12(a)] when calculating the solid angle (Count 2). When this solid angle is ≥ 0.5, the voxel p is classified as a voxel of HBVs and added to the segmented liver [Fig. 12(b)].

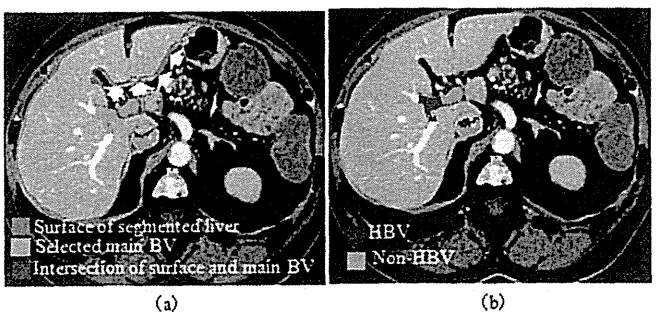

FIG. 12. Refining main BV based on solid angle: (a) an example of the selected region of main BVs (liver surface at the region that is marked with arrows is excluded when calculating solid angles by setting r = 15 mm) and (b) main BV at the selected region are classified into HBVs and non-HBVs (MICCAI-training-15).

2.C.4.b. Filling holes in 3D. Holes are filled in 3D to avoid undersegmentation. In this step, when a hole is surrounded by NLIT, it is filled and added to the NLIT. Whereas, when the hole is surrounded by an LIT, it is filled and added to the LIT. Holes that are surrounded by LIT and NLIT are filled and added to the NLIT (liver). To smooth the surface of the segmented liver, an opening operation is applied with a radius of 1 mm.

3. RESULTS

MICCAI-test and non-MICCAI databases are used to evaluate the precision of the proposed method. Segmented livers were compared with their corresponding references. Five measures of accuracy from the MICCAI workshop for liver segmentation in 2007 were applied for all segmentation results. These measures are based on volumetric overlap and surface distances, and calculated as in Heimann *et al.*[3] These measures are volumetric overlap error (VOE), relative volume difference (RVD), average symmetric surface distance (ASD), root mean square symmetric distance (RMSD), and maximum symmetric surface distance (MSD). Segmentation is perfect (worth 100 per measure) when each of these measures is zero. The RVD is given as a signed number to show if the method tends to under- or oversegment. In addition to the MICCAI measures, the following volume measures[27] were applied for the non-MICCAI datasets:

- TPVT, in percent = (number of true positive in the segmented image/number of voxels in the liver's reference) $\times$ 100.
- FPVT, in percent = (number of false positive voxels in the segmented image/number of voxels in the liver's reference) $\times$100.

Evaluation of MICCAI test data was performed by the organizers of the sliver07 website. These organizers applied the same tools and scoring system that they used in the MICCAI workshop for liver segmentation in 2007, and this tool calculates the same five measures as sliver07. These results are summarized in Table I with an overall score of 85.7, which ranks best among results on the site as of July 2013.

The precision of the method was also evaluated by applying the same measures and other standard measures to the results obtained from non-MICCAI data, as illustrated in Table II. Tables I and II demonstrate the usefulness of the proposed method at segmenting livers form MICCAI and non-MICCAI databases.

Our study found the processing time (average $\pm$ SD) for extracting and classification of BVs to be 4.6 $\pm$ 0.9 min when applied by an experienced user. The user with low experience may need one minute more for correction of

TABLE I. Evaluation of the method performance based on MICCAI test data results was obtained by the organizers of sliver07 website using the same tools and scoring system that were used in the 2007 MICCAI workshop (SD: standard deviation).

Measure	VOE		RVD		ASD		RMSD		MSD		
Test case	(%)	Score	(%)	Score	(mm)	Score	(mm)	Score	(mm)	Score	Total score
1	4.3	83.2	1.02	94.6	0.58	85.6	1.02	85.8	10.12	86.7	87.2
2	4.19	83.6	-0.78	95.9	0.58	85.4	1.36	81	17.62	76.8	84.6
3	4.28	83.3	1.16	93.9	0.8	79.9	1.27	82.4	17.65	76.8	83.2
4	4.72	81.6	−0.3	98.4	0.68	83	1.38	80.8	15.4	79.7	84.7
5	5.33	79.2	−0.26	98.6	0.87	78.3	1.55	78.4	15.88	79.1	82.7
6	3.81	85.1	−0.67	96.4	0.54	86.5	1.07	85.1	11.99	84.2	87.5
7	3.11	87.9	0.41	97.8	0.41	89.8	0.84	88.3	9.43	87.6	90.3
8	4.53	82.3	0.91	95.1	0.69	82.7	1.38	80.9	15.24	79.9	84.2
9	3.6	85.9	1.68	91	0.39	90.2	0.66	90.8	13.02	82.9	88.2
10	5.46	78.7	−0.35	98.1	0.73	81.8	1.32	81.6	13.7	82	84.4
Average	4.33	83.1	0.28	96	0.63	84.3	1.19	83.5	14.01	81.6	85.7
SD	0.73	2.84	0.87	2.42	0.16	3.93	0.28	3.88	2.88	3.79	2.46

interactions' results. The time for segmenting the liver stage was 6.8 ± 1.7 min; here, studied cases had 232 ± 114.6 slices. This was observed when applying the proposed method using a standard computer (Dell Precision T3500, 2.67 GHz Intel Xeon® W3520 CPU, 6.00 GB RAM, Windows Vista™ Business operating system). Processing time can be further decreased through the use of multithread processing.

A visual comparison between segmented livers and their corresponding reference data is shown in Fig. 13.

A review of the proposed method performance on healthy and unhealthy cases of both MICCAI-test and non-MICCAI data are presented in Table III. In order to verify the hypotheses that the method performance does not defer when applied to different datasets, p-values (p) from a nonparametric test[58] (Wilcoxon-Mann-Whitney rank sum test) are calculated based on the MICCAI-test and non-MICCAI data for the five measures of evaluation and are presented in Table IV. Through Tables III and IV, it can be noticed that there is no significant difference ($p > 0.05$) between the performances of the method when applied to healthy and unhealthy datasets. Whereas, the results that were obtained based on non-MICCAI data are significantly ($p < 0.05$) more accurate than the corresponding results that were obtained based on MICCAI-test data. MICCAI-data were scanned using a variety of scanners and scanning conditions[3,48] whereas non-MICCAI data were scanned using the same scanner with a relatively high resolution. The use of newer CT scanners is expected to result in higher-resolution images; consequently, the performance outcomes of the proposed method are expected to be much higher with recent CT scanners than the scanners used in this study.

TABLE II. Evaluation of the method performance using 50 non-MICCAI datasets according to MICCAI workshop measures and other standard measures. Results represent average and standard deviation (SD) of the overall data. Measures are calculated as in Ref. 3.

Measure (unit)	TPVF (%)	FPVF (%)	VOE (%)	RVD (%)	ASD (mm)	RMSD (mm)	MSD (mm)
Average	97.56	1.35	3.21	0.06	0.45	0.98	12.69
SD	1.05	0.82	0.75	1.29	0.17	0.26	3.89

4. DISCUSSION

4.A. Addressing the wide variability in liver shapes and sizes

Our proposed method is based on BV anatomy, which is unique to each scanned liver because of the considerable shape and size variability of livers; this method is thus quite valuable for addressing this wide variability in liver anatomy. In Table V, the average volume over all reference datasets is 1 281 132 mm^3, with an SD of 645 925. This large SD reflects the wide variability of the sizes of livers used in this study. The utility of the proposed method for addressing this variability is reflected in the strong correlation [correlation coefficient (CC) = 0.9988] between reference and segmented livers overall, using the MICCAI training as well as non-MICCAI data [Fig. 14(a)]. This capability is also reflected in the strong correlation (CC = 0.9995) between liver reference and overlapping regions [Fig. 14(b)].

4.B. Separating the liver from other organs

In several approaches (Refs. 23, 24, 27, 38, 39, and 41) for segmenting the liver from the portal phase of a CT dataset, the liver could not be separated from its neighboring organs of similar intensity. Our proposed method successfully segments the liver without interference from other nearby organs. This is achieved based on (1) variation in intensity between the liver and its neighboring organs and (2) constructing a boundary surface based on core region and non-HBVs cluster [Sec. 2.C.2 (Step 2)].

Variation in intensity is applied by using the range of extension that is decided based on the components of the core region histogram. This core region intensity is higher when compared with neighboring organs such as the gallbladder,

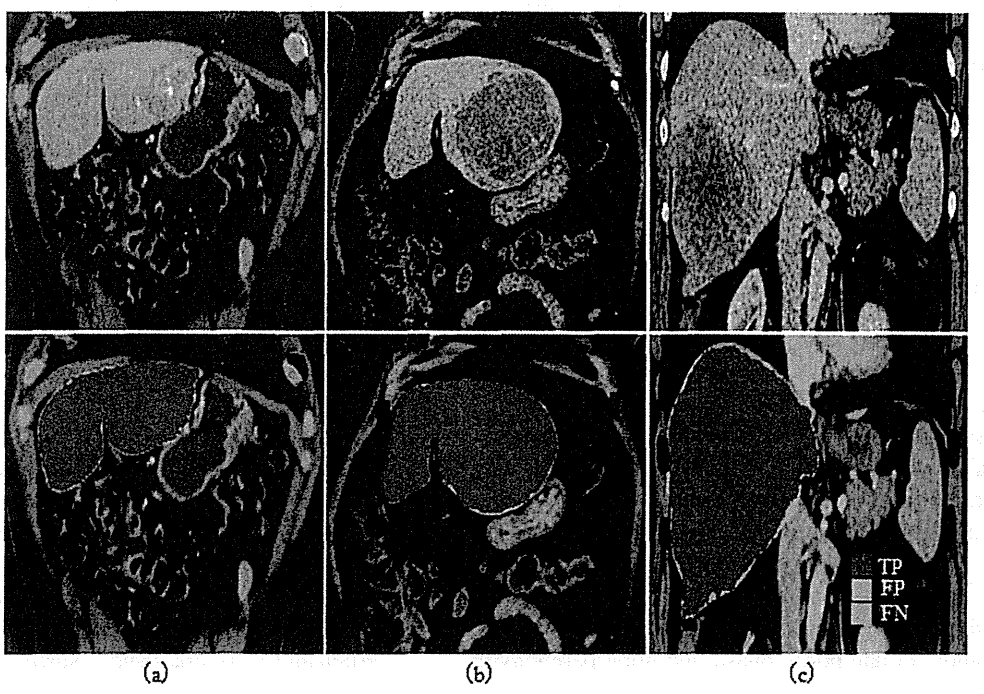

FIG. 13. Evaluation of segmented livers on scans containing severe pathological abnormalities. Although abnormalities, segmented livers agree with their references. (a) Large tumor with high intensity, (b) large LIT (non-MICCAI data), (c) large LIT (MICCAI training 16). (Up) Original dataset and (down) results of overlapping both segmented livers and their references are illustrated.

the stomach, surrounding muscles, air regions, etc. Bones are also separated based on variation in intensity with the liver where their intensity is changed into a negative value [Sec. 2.B.1 (Step 1)]. This variation stops segmentation of the liver from leaking into these organs during the extension process. The boundary surface prevents the liver from leaking into neighboring organs having a similar intensity when they are overlaid close to each other during extension of the core region such as the kidneys, the spleen, the heart, the pancreas, the intestines [Figs. 15(a) and 15(b)], and muscles at LIT-cases. As an example, the stomach is usually separated through variation in intensity with liver tissue. However, in the abnormal stomach (i.e., one having high intensity and located overly close to the liver), the stomach is extracted and classified in the non-HBV cluster. The boundary surface then prevents leakage of the liver into the stomach on CT images [Fig. 15(c)].

The gallbladder sits just beneath the liver and has an intensity that is lower than the liver parenchyma, HBVs and mostly LITs. The gallbladder is excluded from the liver core region by applying the intensity condition of Delaunay triangulation [Sec. 2.C.1 (Step 1)]. It is also excluded during extension of the liver based on intensity variation of histogram components. In LIT-livers, the NLIT-core region is extended first and stops from leaking into the gallbladder based on intensity variations as usual, then this extension result is used to stop LIT-core region extension from leaking into the gallbladder. In some abnormal cases, the gallbladder contains some accumulated calcium. This calcium is extracted with bone and added to the non-HBV cluster [Sec. 2.B.2.c (Step 3)]. Consequently, the boundary surface prevents leakage into the gallbladder [Figs. 8(a) and 8(d)]. This boundary surface is a salient feature of the proposed method.

Muscles are usually separated based on intensity variation with the liver parenchyma. In LIT-cases, muscles have nearly the same intensity of LIT and overlay close to each other [Fig. 16(e)]. Therefore, Muscles are separated from LIT by the constructed boundary surface. To construct this boundary surface, the ribs boundary surface [Sec. 2.B.2.c (Step 3)] is added to the non-HBVs cluster to set the boundary surface inside ribs cage. This ribs boundary surface could effectively solve the problem of separating muscles form the LITs neighboring the ribs cage. Muscles on the inner surface of the liver are separated from neighboring LITs by the boundary surface.

TABLE III. Comparison of the performance of the proposed method based on healthy and unhealthy cases of MICCAI-test and non-MICCAI data. Results are presented as "averages ± standard deviations."

	Measure (Unit)	VOE (%)	RVD (%)	ASD (mm)	RMSD (mm)	MSD (mm)
MICCAI-test data	Healthy	4.2 ± 0.9	0.4 ± 0.9	0.6 ± 0.2	1.2 ± 0.4	14.2 ± 3.2
	Unhealthy	4.5 ± 0.6	0.2 ± 0.9	0.7 ± 0.1	1.2 ± 0.2	13.8 ± 2.9
Non-MICCAI data	Healthy	3.4 ± 0.9	0.4 ± 1.3	0.45 ± 0.2	0.9 ± 0.2	12.1 ± 3.3
	Unhealthy	2.9 ± 0.6	−0.1 ± 1.3	0.45 ± 0.2	1.02 ± 0.3	13.1 ± 4.3

TABLE IV. The p-value is obtained using a nonparametric test (Wilcoxon-Mann-Whitney rank sum test).

P-value	MICCAI and non-MICCAI	Healthy and unhealthy
VOE	0.0078[a]	0.2189
RVD	0.0614	0.2154
ASD	0.0206[a]	0.7039
RMSD	0.0688	0.3754
MSD	0.1973	0.8707

[a]Significant at $p < 0.05$.

TABLE V. Volumetry of segmented livers are measured for the MICCAI-training and non-MICCAI datasets. Results are compared with their references and shown as averages and standard deviations (SD) overall data.

	Region (unit)	Segmented liver (mm^3)	Reference (mm^3)	Overlapped (mm^3)
MICCAI-training data	Average	985 574	993 785	965 533
	SD	469 866	478 676	461 697
Non-MICCAI data	Average	1 403 595	1 396 071	1 369 084
	SD	685 589	671 926	670 059
Overall datasets	Average	1 284 160	1 281 132	1 253 784
	SD	656 325	645 925	641 291

However, the part of this muscle that is connected to the LIT and exists inside the boundary surface will be oversegmented (MICCAI-training 16).

In the portal phase, when the difference of intensity between most of the renal parenchyma and the liver is more than 20 HU. The kidney leakage to the liver was few enough not to affect the liver segmentation result. This is from our experience with the 80 datasets (MICCAI and non-MICCAI) used in this study. In late portal phase, the renal parenchyma may have almost same intensity as the liver. In this case, the region growing of kidneys is expected to leak into the liver parenchyma and the user has to separate them manually.

4.C. Segmenting LIT

Several approaches (Refs. 27, 38, and 40–42) for segmenting the liver from the portal phase result in undersegmentation of LITs. The proposed method is effective at segmenting LITs, as it classifies the histogram of the segmented core region of a LIT-liver into two components, one for the NLIT-part and the other for the LIT [Fig. 9(b)]. In a similar manner, the method classifies the core region of this LIT-liver into two partial core regions, one representing the core region of the NLIT-part and the other representing the core region of the LIT [Fig. 16(c)]. Each core region is extended based on its corresponding component [Sec. 2.C.3.b (Step 3.2)] [Fig. 16(d)]. Through reconfirmation of the boundary surface [Sec. 2.C.3.b (Step 3.2)], each contact region of NLIT- and LIT-results [Fig. 16(f)] is re-extended to complete segmentation of the liver [Fig. 16(g)]. In this step, muscles and LITs are mainly separated through stopping the contact region extension by the final boundary surface. During liver segmentation, the method separately identifies the NLIT- and the LIT-parts of LIT-livers in 3D [Fig. 16(h)].

When an LIT is small and is surrounded by BVs, it has two cases: (1) the LIT satisfies the intensity condition of Delaunay triangulation, this LIT is segmented with the core region and consequently with the liver [Figs. 16(a)–16(d) upper tumor]. (2) The LIT does not satisfy the intensity condition, this LIT will be a hole in the liver and will be segmented through filling holes at the refinement step and added to the liver. When a peripheral LIT is small and not surrounded by BVs at all, it will be undersegmented (MICCAI-test 1). Tumors that are small enough not to a distinguished as component in the mixture model will be segmented and classified in the NLIT-part of the liver.

4.D. Inter user variability

To avoid interuser variability, each interaction is followed by an automatic process that corrects this variability. For choosing the seed point of kidneys region growing [Sec. 2.B.1.a (Step 1)], an automatic correction is applied through replacing the chosen seed point by a 2D-region of

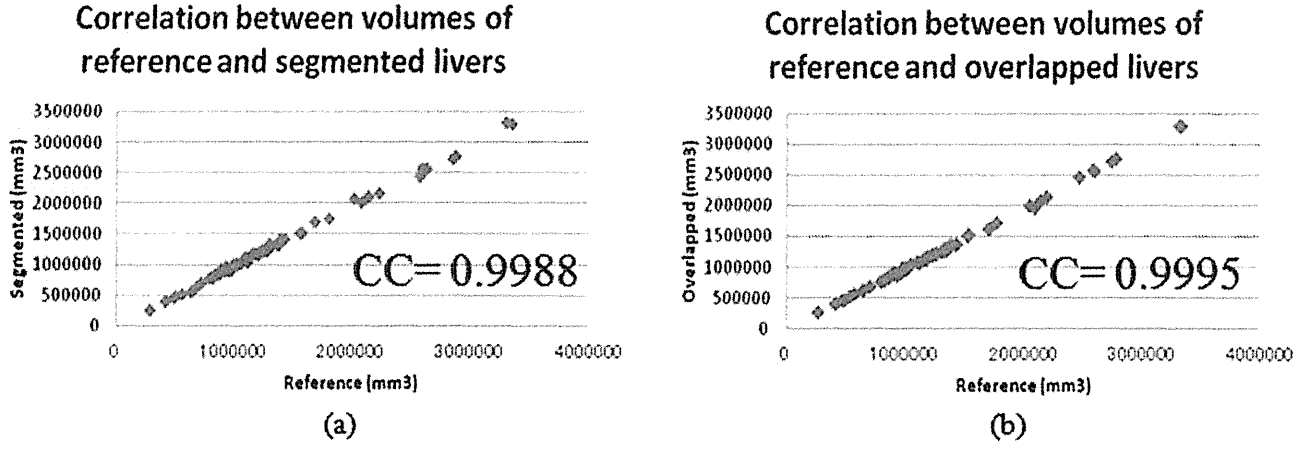

FIG. 14. Analysis of the relationship between segmented livers and their references using MICCAI-training and non-MICCAI data: (a) the correlation between volumes of segmented livers and their references and (b) the correlation between volumes of the overlapped liver regions and their corresponding references.

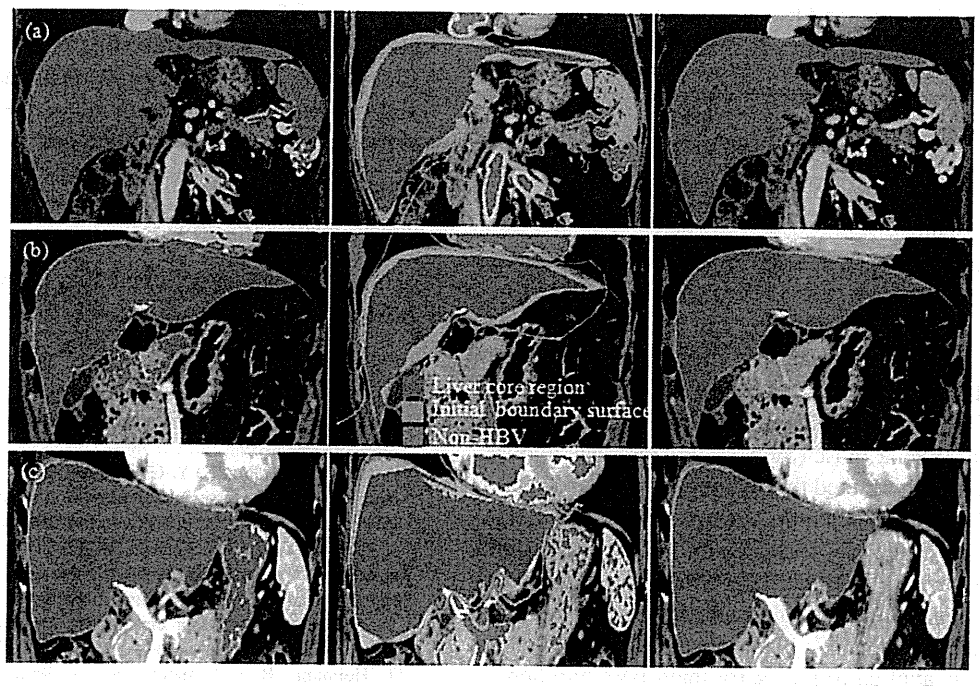

FIG. 15. Effectiveness of the constructed boundary surface at separating different organs neighboring the liver and having a similar intensity. (Left) Liver and other organs before constructing the boundary surfaces are illustrated (only the intensity variation condition is applied). (Middle) Core regions, non-HBVs cluster, and the constructed boundary surface are illustrated. (Right) Liver is separated from other organs in different cases by the boundary surface. (a) The spleen is separated. (b) The heart, pancreas, and intestines are separated in another case. (c) The stomach is separated in a third case (MICCAI - test 7).

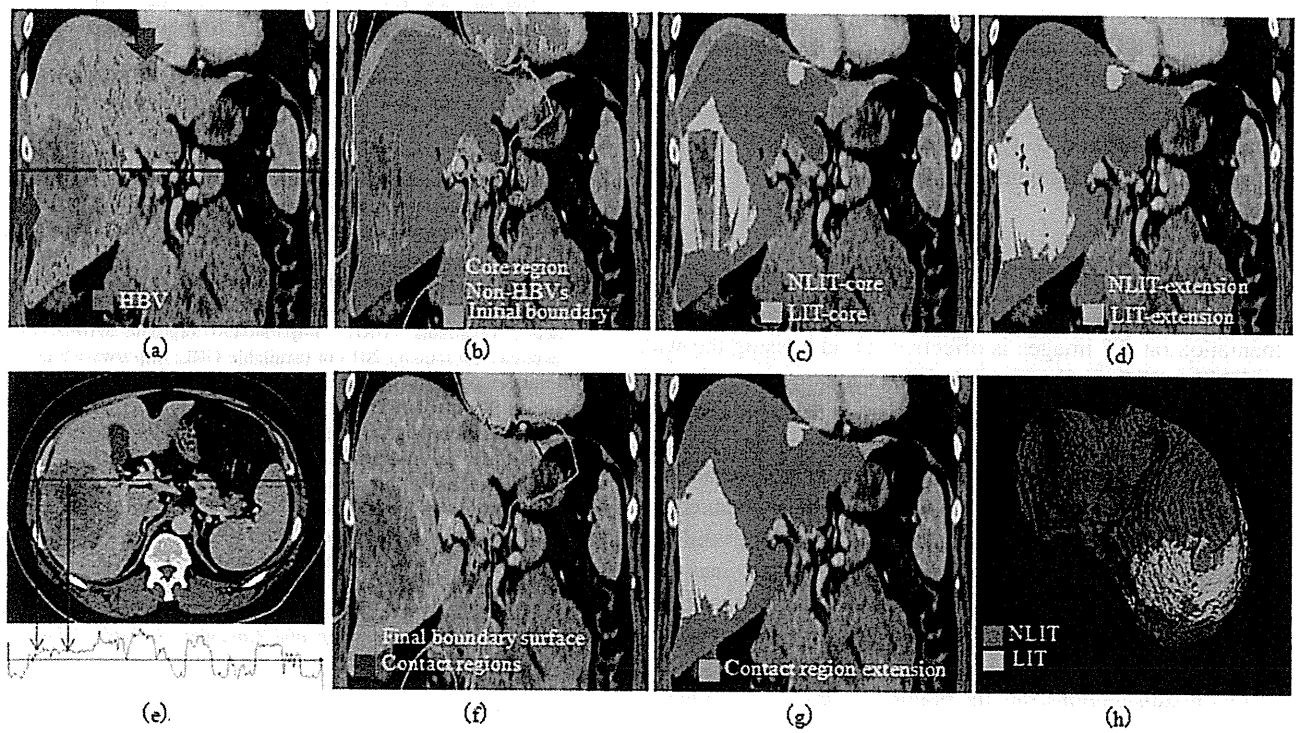

FIG. 16. Segmentation of a liver having a severe LIT: (a) HBVs surrounds the LIT [peripheral LITs are marked with arrows; (left) large LIT and (up) small LIT]. (b) Initial boundary surface is constructed between the core region and non-HBVs cluster. (c) Core region is classified into LIT- and NLIT-core regions. (d) Extensions of LITs and NLIT-cores are stopped by the initial boundary surface and intensity variation. (e) Muscles and LIT have nearly same intensity [position of this slice is marked with line in (a)]. (f) Contact regions of the first extension results and the initial boundary are illustrated with the final boundary surface. (g) The contact region in (f) is re-extended and stopped based on the final boundary and intensity variation. Holes are filled. (h) LIT and NLIT are illustrated in 3D.

TABLE VI. The p-value is measured from the results of two users.

P-value	Two users
VOE	0.1049
RVD	0.1949
ASD	0.1883
RMSD	0.8745
MSD	0.8785

radius 2 mm. Calculating the mean of intensities in this region, this mean is used as the actual threshold for the region growing. In choosing the seed point of blood vessel extraction region growing [Sec. 2.B.1.c (Step 3)], the interuser variability is automatically corrected through replacing the seed point with a 2D-region of radius 6 mm. The histogram of this region is calculated. The intensity corresponding to 75th percentile of these histograms is automatically chosen to be the actual threshold. In separating main blood vessels from abdominal BVs [Sec. 2.B.2.a (Step 1)], blood vessel refinement based on solid angle is applied to reclassify main BVs into hepatic and nonhepatic [Sec. 2.C.4 (Step 4)]. In order to verify the hypotheses that the method performance does not defer when applied by different users, p-value from a nonparametric test was measured for two users as in Table VI. This table demonstrates that the method is stable ($p > 0.05$) against interuser variability.

During reconfirmation of the initial boundary surface, the contact region between the boundary surface and the core region extension result was extended. This extension was stopped by the final boundary surface and intensity variation [Sec. 2.C.3.b (Step 3.2)]. It was noticed that: (1) where the first and the final boundary surfaces overlap, the contact region was not extended. (2) A very little region of the liver was under- or oversegmented.

5. CONCLUSIONS AND FUTURE WORK

This study demonstrates that the use of BVs in liver segmentation on CT images is effective for addressing the wide variability of liver shapes and sizes. Constructing a boundary surface using HBVs and non-HBVs is useful for separating the liver from its neighboring organs of similar intensity. By fitting the histogram of the core region using a variational Bayesian Gaussian mixture model, LIT can be segmented and quantitative measurement of NLIT- and LIT-parts of the liver becomes available. The proposed method's efficacy was evaluated using the standard MICCAI measures for liver segmentation and other standard measures of image segmentation for MICCAI and non-MICCAI data.

Our results demonstrate the potential usefulness of the proposed method for segmenting the liver, and we expect that this method may prove useful information to surgeons planning liver surgery and to other medical professionals working in clinical settings. Specifically, this method may provide important volumetric information about the liver and any associated hepatic tumors. The average processing time of the method is 9.7 min on a standard computer, which can be decreased by using multithreading processing. Based on deeper BV analysis, ABVs can be extracted and classified automatically. Thus, further developing the method so that it is fully automatic may be a worthwhile goal.

ACKNOWLEDGMENTS

This study was supported by a Grant-in-Aid for Scientific Research on Innovative Areas (21103005).

[a]Author to whom correspondence should be addressed. Electronic mail: niki@opt.tokushima-u.ac.jp; Telephone: +81886569430; Fax: +81886569433.

[1]F. Wang, K. T. Pan, S. Y. Chu, K. M. Chan, H. S. Chou, T. J. Wu, and W. C. Lee, "Preoperative estimation of the liver graft weight in adult right lobe living donor liver transplantation using maximal portal vein diameters," Liver Transplant. **17**, 373–380 (2011).

[2]S. Saito, J. Yamanaka, K. Miura, N. Nakao, T. Nagao, T. Sugimoto, T. Hirano, N. Kuroda, Y. Iimuro, and J. Fujimoto, "A novel 3D hepatectomy simulation based on liver circulation: Application to liver resection and transplantation," Hepatology **41**, 1297–1304 (2005).

[3]T. Heimann, B. v. Ginneken, M. A. Styner, Y. Arzhaeva, V. Aurich, C. Bauer, A. Beck, C. Becker, R. Beichel, G. Bekes, F. Bello, G. Binnig, H. Bischof, A. Bornik, P. M. Cashman, Y. Chi, A. Cordova, B. M. Dawant, M. Fidrich, J. D. Furst, D. Furukawa, L. Grenacher, J. Hornegger, D. Kainmüller, R. I. Kitney, H. Kobatake, H. Lamecker, T. Lange, J. Lee, B. Lennon, R. Li, S. Li, H. P. Meinzer, G. Nemeth, D. S. Raicu, A. M. Rau, E. M. V. Rikxoort, M. Rousson, L. Rusko, K. A. Saddi, G. Schmidt, D. Seghers, A. Shimizu, P. Slagmolen, E. Sorantin, G. Soza, R. Susomboon, J. M. Waite, A. Wimmer, and I. Wolf, "Comparison and evaluation of methods for liver segmentation from CT datasets," IEEE Trans. Med. Imaging **28**, 1251–1265 (2009).

[4]T. Heimann and H.-P. Meinzer, "Statistical shape models for 3D medical image segmentation: A review," Med. Image Anal. **13**(4), 543–563 (2009).

[5]P. Campadelli, E. Casiraghi, and A. Esposito, "Liver segmentation from computed tomography scans: A survey and a new algorithm," Artif. Intell. Med. **45**(2–3), 185–196 (2009).

[6]A. Schenk, G. Prause, and H. O. Peitgen, "Efficient semiautomatic segmentation of 3D objects in medical images," in *Proceedings of Medical Image Computing And Computer-Assisted Intervention (MICCAI) 2000*, Lecture Notes in Computer Science Vol. 1935 (Springer-Verlag, Berlin Heidelberg, 2000), pp. 71–131.

[7]A. Wimmar, G. Soza, and J. Hornegger, "Two-stage Semi-automatic Organ Segmentation Framework using Radial Bias Functions and Level sets" (available URL: http://sliver07.org/data/2010-01-14-1941.pdf), accessed 30 January 2013 or (available URL: http://www5.informatik.uni-erlangen.de/Forschung/Publikationen/2007/Wimmer07-TSO.pdf), accessed 30 January 2013.

[8]M. Kobashi and L. G. Shapiro, "Knowledge-based organ identification from CT images," Pattern Recognit. **28**(4), 475–491 (1995).

[9]D.-Y. Tsai and N. Tanahashi, "Neural-network-based boundary detection of liver structure in CT images for 3-D visualization," *Proceedings of IEEE International Conference on Neural Networks, IEEE Catalog No. 04CH37541* (Neural Networks, Orlando, FL, 1994), Vol. 6, pp. 3484–3489.

[10]T. Heimann, I. Wolf, and H. P. Meinzer, "Active shape models for a fully automated 3D segmentation of the liver—An evaluation on clinical data," *Medical Image Computing and Computer Assisted Intervention*, Lecture Notes in Computer Science Vol. 4191 (Springer, Heidelberg, 2006), pp. 41–48.

[11]D. Kainmuller, T. Lange, and H. Lamecker, "Shape Constrained Automatic Segmentation of the Liver based on a Heuristic Intensity Model" (available URL: http://www.sliver07.org/data/2007-10-22-1942.pdf), accessed 6 November 2012.

[12]A. Wimmer, G. Soza, and J. Hornegger, "A Generic Probabilistic Active Shape Model for Organ Segmentation" (available URL: http://www.sliver07.org/data/2009-03-11-0340.pdf), accessed 6 November 2012.

[13]L. Gao, D. G. Heath, and E. K. Fishman, "Abdominal image segmentation using three-dimensional deformable models," Invest. Radiol. **33**(6), 348–355 (1998).

[14]T. Okada, R. Shimada, Y. Sato, M. Hori, K. Yokota, M. Nakamoto, Y.-W. Chen, H. Nakamura, and S. Tamura, "Automated segmentation of the liver from 3D CT images using probabilistic Atlas and multi-level statistical shape model," *MICCAI 2007*, Lecture Notes in Computer Science Vol. 4791 (Springer-Verlag, Berlin Heidelberg, 2007), Part I, pp. 86–93.

[15]A. Wimmer, G. Soza, and J. Hornegger, "A generic probabilistic active shape model for organ segmentation," *MICCAI 2009*, Lecture Notes in Computer Science Vol. 5762 (Springer-Verlag Berlin, Heidelberg, 2009), Part II, pp. 26–33.

[16]J. Peng, "A new convex variational model for liver segmentation," *21st International Conference on Pattern Recognition (ICPR)*, (Pattern Recognition (ICPR), 2012 21st International Conference on, Tsukuba, 2012), pp. 3754–3757.

[17]M. Erdt, M. Kirschner, S. Steger, and S. Wesarg, "Fast automatic liver segmentation combining learned shape priors with observed shape Deviation," in *Proceedings of the IEEE International Symposium on Computer-Based Medical Systems (CBMS)* (Computer-Based Medical Systems (CBMS), 2010 IEEE 23rd International Symposium on, Perth, WA, 2010), pp. 249–254.

[18]K. Drechsler and C. O. Laura, "Simulation of portal vein clamping and the impact of safety margins for liver resection planning," *Abdominal Imaging. Computational and Clinical Applications Workshop Held on Conjunction with MICCAI 2011*, Lecture Notes in Computer Science Vol. 7029 (Springer-Verlag, Berlin Heidelberg, 2012), pp. 149–156.

[19]X. Zhou, T. Kitagawa, T. Hara, H. Fujita, X. Zhang, R. Yokoyama, H. Kondo, M. Kanematsu, and H. Hoshi, "Constructing a probabilistic model for automated liver region segmentation using non-contrast X-Ray TorsoCT images," *MICCAI 2006*, Lecture Notes in Computer Science Vol. 4191 (Springer-Verlag, Berlin Heidelberg, 2006), pp. 856–863.

[20]H. Park, P. H. Bland, and C. R. Meyer, "Construction of an abdominal probabilistic atlas and its application in segmentation," IEEE Trans. Med. Imaging **22**(4), 483–492 (2003).

[21]D. Furukawa, A. Shimizu, and H. Kobatake, "Automatic liver segmentation method based on maximum a posterior probability estimation and level set method," in *MICCAI 2007 Workshop Proceedings of the 3D Segmentation in the Clinic: A Grand Challenge* (2007), pp. 117–124.

[22]M. G. Linguraru, J. K. Sandberg, Z. Li, F. Shah, and R. M. Summers, "Automated segmentation and quantification of liver and spleen from CT images using normalized probabilistic atlases and enhancement estimation," Med. Phys. **37**(2), 771–783 (2010).

[23]L. Fernandez-de-Manuel, J. L. Rubio, M. J. Ledesma-Carbayo, J. Pascau, J. M. Tellado, E. Ramon, M. Desco, and A. Santos, "3D liver segmentation in preoperative CT images using a level-sets active surface method," Conf. Proc. IEEE Eng. Med. Biol. Soc. **2009**, 3625–3628 (2009).

[24]J. Lee, N. Kim, H. Lee, J. B. Seo, H. J. Won, Y. M. Shin, Y. G. Shin, and S. H. Kim, "Efficient liver segmentation using a level-set method with optimal detection of the initial liver boundary from level-set speed images," Comput. Methods Programs Biomed. **88**(1), 26–38 (2007).

[25]S. Pan and B. M. Dawant, "Automatic 3D segmentation of the liver from abdominal CT images: A level-set approach," Proc. SPIE **4322**, 128–138 (2001).

[26]R. Susomboon, D. S. Raicu, and J. Furst, "A hybrid approach for liver segmentation," in *Proceedings of MICCAI Workshop on 3D Segmentation in the Clinic: A Grand Challenge* (2007), pp. 151–160.

[27]L. Ruskó, G. Bekes, and M. Fidrich, "Automatic segmentation of the liver from multi- and single-phase," Med. Image Anal. **13**(6), 871–882 (2009).

[28]Y. Y. Boykov and M.-P. Jolly, "Interactive graph cuts for optimal boundary & region segmentation of objects in N-D images," Proc. Int. Conf. Comput. Vis. **I**, 105–112 (2001).

[29]Y. Boykov and G. Funka-Lea, "Graph cuts and efficient N-D image segmentation," Int. J. Comput. Vis. **70**(2), 109–131 (2006).

[30]R. Beichel, C. Bauer, A. Bornik, E. Sorantin, and H. Bischof, "Liver segmentation in CT data: A segmentation refinement approach," *3D Segmentation in the Clinic: A Grand Challenge* (2007), pp. 235–245.

[31]A. Afifi and T. Nakaguchi, "Liver segmentation approach using graph cuts and iteratively estimated shape and intensity constrains," *Proceedings of the 15th Conference on Medical Image Computing and Computer-Assisted Intervention (MICCAI)* (Springer-Verlag, Berlin Heidelberg, 2012), Pt. 2, pp. 395–403.

[32]L. Massoptier and S. Casciaro, "Fully automatic liver segmentation through graph-cut technique," *Proceedings of the 29th Annual International Conference of the IEEE -EMBS* (Engineering in Medicine and Biology Society, 2007, EMBS 2007, 29th Annual International Conference of the IEEE, Lyon, 2007), pp. 5243–5246.

[33]S. Esneault, N. Hraiech, E. Delabrousse, and J.-L. Dillenseger, "Graph cut liver segmentation for interstitial ultrasound therapy," *Conference Proceedings of the International Conference of IEEE Engineering in Medicine and Biology Society* (Engineering in Medicine and Biology Society, 2007, EMBS 2007, 29th Annual International Conference of the IEEE, Lyon, 2007), pp 5247–5250.

[34]Y. Chen, W. Zhao, Q. Wu, Z. Wang, and J. Hu, "Liver segmentation in CT images for intervention using a graph-cut based model," *Abdominal Imaging. Computational and Clinical Applications Workshop Held on Conjunction with MICCAI 2011*, Lecture Notes in Computer Science Vol. 7029 (Springer-Verlag, Berlin Heidelberg, 2012), pp. 157–164.

[35]M. G. Linguraru, W. J. Richbourg, J. M. Watt, V. Pamulapati, and R. M. Summers, "Liver and tumor segmentation and analysis from CT of diseased patients via a generic affine invariant shape parameterization and graph cuts," *Abdominal Imaging 2011*, Lecture Notes in Computer Science Vol. 7029 (Springer-Verlag, Berlin Heidelberg, 2012), pp. 198–206.

[36]V. Pamulapati, A. Venkatesan, B. J. Wood, and M. G. Linguraru, "Liver segmental anatomy and analysis from vessel and tumor segmentation via optimized graph cuts," *Abdominal Imaging 2011*, Lecture Notes in Computer Science Vol. 7029 (Springer-Verlag, Berlin Heidelberg, 2012), pp 198–206.

[37]M. G. Linguraru, W. J. Richbourg, J. Liu, J. M. Watt, V. Pamulapati, S. Wang, and R. M. Summers, "Tumor burden analysis on computed tomography by automated liver and tumor segmentation," IEEE Trans. Med. Imaging **31**(10), 1965–1976 (2012).

[38]D. A. Oliveira, R. Q. Feitosa, and M. M. Correia, "Segmentation of liver, its vessels and lesions from CT images for surgical planning," Biomed. Eng. Online (available URL: http://www.biomedical-engineering-online.com/content/10/1/30), accessed 30 September 2013.

[39]S.-J. Lim, Y.-Y. Jeong, and Y.-S. Ho, "Automatic liver segmentation for volume measurement in CT Images," Vis. Commun. Image Represent. **17**(4), 860–875 (2006).

[40]G. Schmidt, M. Athelogou, R. Schönmeyer, R. Korn, and G. Binnig, "Cognition network technology for a fully automated 3D segmentation of liver," in *MICCAI 2007 Workshop Proceedings of the 3D Segmentation in the Clinic: A Grand Challenge* (2007), pp. 125–134.

[41]K. A. Saddi, M. Rousson, C. C. hotel, and F. Cheriet, Global-to-local shape matching for liver segmentation in CT imaging. in *MICCAI 2007 Workshop Proceedings of the 3D Segmentation in the Clinic: A Grand Challenge* (2007), pp. 207–214.

[42]W. N. J. W. Yussof and H. Burkhardt, "Automatic 3D liver segmentation using morphological operations and graph-cut techniques," Journal of Next Generation Information Technology **2**(3), 23–34 (2011).

[43]A. S. Maklad, M. Matsuhiro, H. Suzuki, Y. Kawata, N. Niki, T. Utsunomiya, and M. Shimada, "Blood vessel-based liver segmentation through the portal phase of a CT dataset," Proc. SPIE **8670**, 86700X-1–86700X-7 (2013)

[44]A. S. Maklad, M. Matsuhiro, H. Suzuki, Y. Kawata, N. Niki, T. Utsunomiya, and M. Shimada, "Extraction of liver volumetry based on blood vessel from the portal phase CT dataset," Proc. SPIE **8314**, 83142O-1–83142O-7 (2012).

[45]T. Saitoh, Y. Tamura, and T. Kaneko, "Automatic segmentation of liver region based on extracted blood vessels," Syst. Comput. Jpn. **35**(5), 1–10 (2004) [Denshi Joho Tsushin Gakkai Ronbunshi **J86-D-II**(5), 633–641 (2003)].

[46]I. R. Francis, R. H. Cohan, N. J. McNulty, J. F. Platt, M. Korobkin, A. Gebremariam, and K. I. Ragupathi, "Multidetector CT of the liver and hepatic neoplasms: Effect of multiphasic imaging on tumor conspicuity and vascular enhancement," AJR, Am. J. Roentgenol. **180**(5), 1217–1224 (2003).

[47]A. Oto, K. Kulkarni, R. Nishikawa, and R. L. Baron, "Contrast enhancement of hepatic heangiomas on multiphase MDCT: Can we daiagnose hepatic hemangiomas by comparing enhancement with blood pool?," AJR, Am. J. Roentgenol. **195**(2), 381–386 (2010).

[48]B. V. Ginnekan, T. Heimann, and M. Styner, "3D Segmentation in the clinic: A grand challenge," in *MICCAI 2007 Workshop Proceedings of the 3D Segmentation in the Clinic:A Grand Challenge* (American Roentgen Ray Society, 2007), pp 7–15.

[49]I. Pitas, *Digital Image Processing Algorithms and Applications* (Wily Inter Science, U.S.A., 2000).

[50]A. Fabijanska "Results of applying a two-path region growing algorithm for airway tree segmentation to MDCT chest scans from EXACT database," *EXACT09* (2009), pp. 251–260 (available URL: http://image.diku.dk/exact/result/VOLCED_description.pdf), accessed 2 July 2013.

[51]S. W. Smith, *The Scientist and Engineer's Guide to Digital Signal Processing*, 2nd ed., (California Technical Publishing, San Diego, 1997–2011), Chap. 25, pp 436–442 (available URL: http://www.dspguide.com/CH25.PDF), accessed 9 October 2012.

[52]J. Toriwaki and H. Yoshida, *Fundamentals of Three-Dimensional Digital Image Processing* (Springer-Verlag London Limited, 2009), Sec. 5.

[53]E. Takahashi, Y. Kawata, N. Niki, Y. Nakano, M. Harada, and N. Moriyama, "Computer aided diagnosis for osteoporosis based on vertebral column structure analysis," Proc. SPIE **8315**, 831533 (2012).

[54]D. F. Watson, "Computing the n-dimensional Delaunay tessellation with application to Voronoi polytopes," Comput. J. **24**(2), 167–172 (1981).

[55]K. Palágyi, J. Tschirren, E. A. Hoffman, and M. Sonka, "Quantitative analysis of pulmonary airway tree structures," Comput. Biol. Med. **36**(9), 974–996 (2006).

[56]C. M. Bishop, *Pattern Recognition and Machine Learning* (Springer Science+Business Media, LLC, Singapore), Sec. 10.

[57]S. O'Brien, "Computing the Solid Angle of Two Detectors Using Monte Carlo Methods" (available URL: http://acadine.physics.jmu.edu/group/technical_notes/Solid_angle_latex/solid_angle.pdf), accessed 18 December 2012.

[58]P. Dalgaard, *Statistics and Computing: Introductory Statistics with R* (Springer-Verlag, New York, 2002).

Cancer Chemother Pharmacol (2013) 72:463–470
DOI 10.1007/s00280-013-2222-x

ORIGINAL ARTICLE

A multi-institutional phase II trial of hepatic arterial infusion chemotherapy with cisplatin for advanced hepatocellular carcinoma with portal vein tumor thrombosis

Masafumi Ikeda · Takuji Okusaka · Junji Furuse · Shuichi Mitsunaga · Hideki Ueno · Hidekazu Yamaura · Yoshitaka Inaba · Yoshito Takeuchi · Mitsuo Satake · Yasuaki Arai

Received: 11 February 2013 / Accepted: 16 June 2013 / Published online: 29 June 2013

Abstract
Purpose The objective of this study was to evaluate the response rate, survival, and adverse effects of hepatic arterial infusion chemotherapy (HAIC) using cisplatin in patients with advanced hepatocellular carcinoma (HCC) and portal vein tumor thrombosis (PVTT).
Methods Twenty-five patients of advanced HCC with PVTT in the main or first branch, having no prior history of chemotherapy, measurable lesions, adequate liver and renal function, and adequate bone marrow reserve, were enrolled. Cisplatin was administered at the dose of 65 mg/m^2 via the proper hepatic artery. Treatment was repeated every 4–6 weeks for a maximum of six courses until the appearance of evidence of tumor progression or unacceptable toxicity.
Results The median number of treatments was 3 (range 1–6). Among the 25 enrolled patients, complete response was achieved in 1 (4 %) patient and partial response in 6 (24 %), corresponding to a response rate of 28 % (95 % CI 12–49 %). The median progression-free and overall survival times and the 1-, 2-, and 3-year survival rates in the enrolled patients were 3.6 and 7.6 months and 40.3, 36.0, 20 %, respectively. Four of the seven patients who showed complete or partial response survived for more than 3 years. The main grade 3/4 non-hematological adverse events of this treatment were elevation of the serum aspartate aminotransferase (44 %) and alanine aminotransferase (24 %).
Conclusion HAIC with cisplatin exerts moderate activity with mild toxicity in advanced HCC patients with PVTT. Especially, markedly prolonged survival can be expected in patients who respond to this treatment.

Keywords Hepatocellular carcinoma · Hepatic arterial infusion chemotherapy · Tumor thrombosis · Cisplatin · Clinical trial

Abbreviations

HCC	Hepatocellular carcinoma
PVTT	Portal vein tumor thrombosis
HAIC	Hepatic arterial infusion chemotherapy
AFP	Alpha-fetoprotein
PIVKA II	Protein induced by vitamin K absence or antagonist-II
AST	Aspartate aminotransferase
ALT	Alanine aminotransferase

M. Ikeda · T. Okusaka · H. Ueno
Hepatobiliary and Pancreatic Oncology Division, National Cancer Center Hospital, Tokyo, Japan

M. Ikeda (✉) · J. Furuse · S. Mitsunaga
Division of Hepatobiliary and Pancreatic Oncology, National Cancer Center Hospital East, Kashiwa, Japan
e-mail: masikeda@east.ncc.go.jp

J. Furuse
Department of Internal Medicine, Medical Oncology, Kyorin University School of Medicine, Tokyo, Japan

H. Yamaura · Y. Inaba
Department of Interventional and Diagnostic Radiology, Aichi Cancer Center, Nagoya, Japan

Y. Takeuchi · Y. Arai
Division of Diagnostic Radiology, National Cancer Center Hospital, Tokyo, Japan

M. Satake
Division of Diagnostic Radiology, National Cancer Center Hospital East, Kashiwa, Japan

Introduction

For advanced hepatocellular carcinoma (HCC) patients with portal vein tumor thrombosis (PVTT), chemotherapy remains one of the most important treatment modalities [1–4]. Sorafenib, an oral multikinase inhibitor targeting Raf kinase and receptor tyrosine kinases, has been acknowledged as the standard agent for advanced HCC [5, 6]. However, it has yielded rather unsatisfactory results in terms of the response and survival in patients with advanced HCC [7, 8]. Hepatic arterial infusion chemotherapy (HAIC), which can increase the local concentration of anticancer drugs with reduced systemic distribution, may be expected to exert better antitumor efficacy and lesser toxicity [9, 10]. Although promising results of HAIC have been reported for advanced HCC with PVTT [11–20], no chemotherapeutic agent or regimen has yet been shown to confer a survival benefit sufficient for adoption as standard therapy.

Cisplatin, which is a heavy metal (platinum) ion complex compound that exerts cytotoxicity by binding to double-stranded DNA, is widely used as one of the chemotherapeutic agents in transcatheter arterial embolization [21–23]. Cisplatin in the form of a fine powder suitable for hepatic artery infusion (IA-call®, Nippon Kayaku Co., Ltd.) has been developed in Japan. Since the solubility of this agent is 2.86 times higher than that of standard cisplatin, the injection time can be shortened. In a phase II trial, administration of this agent by intra-arterial injection over 20–40 min at the dose of 65 mg/m^2 in repeated doses at 4- to 6-week intervals was shown to yield favorable results (response rate 33.8 %) [24]. However, the efficacy of this regimen for advanced HCC with PVTT has not yet been fully evaluated. Therefore, we conducted a multicenter phase II trial to evaluate the efficacy and safety of HAIC with cisplatin in HCC patients with PVTT in the main and/or first branch.

Patients and methods

Eligibility

Patients eligible for study entry had advanced HCC with PVTT. The eligibility criteria were as follows: HCC confirmed by histological examination or liver tumor with a radiological hallmark of HCC and elevation of the serum α-fetoprotein (AFP) levels to ≥400 ng/mL; tumor thrombosis in the main and/or first portal vein; unsuitable candidate for surgical resection; age 20 years or over; Eastern Cooperative Oncology Group performance status of 0–2; measurable disease; interval of 4 weeks or over between the last treatment and the present therapy, and no influence of previous treatments; adequate hematological function (hemoglobin ≥9.0 g/dL, leukocytes ≥3,000/mm^3, and platelets ≥50,000/mm^3), adequate hepatic function [Child-Pugh classification of A or B, serum total bilirubin ≤2.0 mg/dL, and serum aspartate aminotransferase (AST)/alanine aminotransferase (ALT) ≤150 U/L], adequate renal function (serum creatinine ≤1.1 mg/dL); availability of written informed consent.

The exclusion criteria were as follows: prior chemotherapy with cisplatin for HCC, prior radiotherapy, transcatheter arterial chemoembolization or intra-arterial chemotherapy for PVTT, refractory pleural effusion or ascites, no distant metastases, allergic reaction to iodine contrast medium, severe renal, heart or mental disease, active infection, excluding hepatitis B or C viral infection, active concomitant malignancy, pregnant and lactating females; females of childbearing age unless using effective contraception.

The pretreatment evaluation consisted of a complete history and physical examination and baseline assessments of organ function. In addition, dynamic computed tomography of the abdomen and chest radiography were performed for pretreatment staging to assess the local extent of the tumor and exclude the presence of distant metastasis. The number of tumors and tumor distribution were examined by computed tomography and/or angiography. This phase II study was conducted with the approval of each institutional review board and conducted in accordance with the Declaration of Helsinki.

Treatment procedure

Following conventional visceral angiography, HAIC was performed by introducing a angiographic catheter into the proper, right or left hepatic artery, or another feeding artery, and injection of cisplatin at the dose of 65 mg/m^2 over 20–40 min by Seldinger's technique, not using implanted port system for hepatic arterial infusion chemotherapy. Until the appearance of evidence of tumor progression and/or unacceptable toxicity, the treatment was repeated every 4–6 weeks for a maximum of six cycles. Neither lipiodol nor gelatin sponge was allowed in the protocol treatments. Antiemetic prophylaxis with a 5-HT3 antagonist (granisetron 1 mg) plus dexamethasone 8 mg was used at the attending physician's discretion. Patients received adequate hydration and/or diuretics for protection against cisplatin-induced renal dysfunction, and the urine output was carefully monitored, especially during the first 3 days after intra-arterial administration of cisplatin. The cisplatin dose was reduced in case of grade 4 hematological adverse events or serious events had developed during the previous cycle. Patients who were refractory to this treatment regimen were allowed to

receive other anticancer treatments at the attending physician's discretion.

Response and toxicity assessment

The antitumor effect was assessed by intravenous contrast enhanced computed tomography or magnetic resonance imaging every 4–6 weeks. Responses were evaluated according to the WHO criteria [25]. The best overall response was recorded for each patient. The duration of response was defined as the interval from the onset of partial response until the first evidence of disease progression or death. Basic laboratory tests, including a complete blood count with differential leukocyte count, and serum chemistry were performed at least once every 2 weeks during this treatment. The treatment-related adverse events were assessed using the Common Terminology Criteria for Adverse Events, v2.0. Serum levels of AFP and protein induced by vitamin K absence or antagonist-II (PIVKA II) were measured every 4–6 weeks. In patients with a pretreatment AFP level of $\geq$100 ng/mL and of PIVKAII of $\geq$100 mAU/mL, the AFP and PIVKAII responses were assessed; a positive response was defined as a >50 % reduction from the pretreatment level. Progression-free survival was defined as the time from the date of initial treatment to the first documentation of progression or death. Overall survival was measured from the date of initial treatment to the date of death or the date of the last follow-up. The progression-free survival and overall survival curves were calculated by the Kaplan–Meier method.

Statistical considerations

The primary endpoint of this trial was the response rate, and the secondary endpoints were adverse events, progression-free survival, and overall survival. The number of patients enrolled was planned using a two-step design [26] based on an expected response rate of 30 %, a response rate corresponding to no activity of 10 %, α error of 10 %, and β error of 10 %. An interim analysis was planned after 15 patients had been enrolled. If zero or one of the first 15 patients showed a partial response or complete response, the study was to be ended. If a response was detected in more than one of the first 15 patients studied, an additional 10 patients were to be enrolled in a second stage of accrual for more precise estimation of the actual response rate. If a response was detected in more than five of the 25 patients studied, this treatment was considered to be effective. This population was defined as including any patients who received at least one course of study medication. The trial was registered at UMIN-CTR (http://www.umin.ac.jp/ctr/index-j.htm), identification number (UMIN000000488).

Results

Patient characteristics

Twenty-five patients were enrolled in this trial between January 2005 and April 2007 at 3 institutions in Japan, because four patients showed partial response among the first 15 patients in the interim analysis. The characteristics of all the 25 patients are shown in Table 1. There were 20 males and five females, with a median age of 67 (range 47–79) years. Hepatitis B surface antigen and hepatitis C virus antibody were positive in 4 patients (16 %) and 15 patients (60 %), respectively. There were 17 (68 %) patients and 8 (32 %) patients with Child-Pugh class A and B, respectively. Portal vein invasion was noted in the main vein and the first branch in 19 patients (76 %) and 6 (24 %) patients, respectively.

A total of 83 courses were given, with a median of three courses (range 1–6) per patient. The median dose of cisplatin per treatment was 100 mg (range 85–130 mg). The reasons for treatment discontinuation were completion of treatment (6 courses) in 5 patients (20 %), disease progression in 16 patients (64 %), rupture of esophageal varices in 1 patient (4 %), hepatic failure in 1 patient (4 %), and accidental perforation of the colon in 1 patient (4 %). As subsequent treatments, 15 patients did not receive any treatments and the remaining 10 patients received further treatment: HAIC with epirubicin (4 patients), HAIC with interferon plus 5-fluorouracil (5-FU) (1 patient), HAIC with cisplatin (2 patients who had shown disease progression after the termination of 6 cycles of HAIC with cisplatin), and transcatheter arterial chemoembolization with epirubicin (2 patients).

Treatment efficacy

Of the 25 patients, 24 were evaluable for response; the remaining one patient (4 %) could not be evaluated because of early discontinuation of this protocol treatment. One patient (4 %) showed complete response, and 6 (24 %) showed partial response, corresponding to an overall response rate of 28 % (95 % CI 12–49 %); the mean duration of the response was 7.9 months (range 1.4–19.5 months). Eleven patients (44 %) showed stable disease and 5 patients (20 %) showed progressive disease. During the treatment, the serum AFP level decreased by more than 50 % in 7 (44 %) of the 16 patients with a pretreatment level of $\geq$100 U/mL, and the serum PIVKA II level decreased by more than 50 % in 15 (68 %) of the 22 patients with a pretreatment level of $\geq$100 mAU/mL.

At the time of the analysis, 21 patients developed tumor progression; among the remaining 4 patients, the tumor progression status could not be confirmed in 3 patients (on

Table 1 Patient characteristics ($n = 25$)

Characteristics	Number of patients	%
Age (years)		
Median	67	
Range	47–79	
Sex		
Male	20	80
Female	5	20
Eastern Cooperative Oncology Group performance status		
0	21	84
1	4	16
Hepatitis B surface antigen		
Positive	4	16
Hepatitis C antibody		
Positive	15	60
Child-Pugh classification		
A	17	68
B	8	32
Prior treatments		
Present	13	52
Resection	4	16
Local ablation	5	20
TACE	10	40
Portal vein invasion		
Main	19	76
First branch	6	24
Tumor distribution		
Unilateral	8	32
Bilateral	17	68
Ascites		
Present	6	24
Alpha-fetoprotein (ng/mL)		
Median	1,075	
Range	11.3–386,300	
PIVKAII (mAU/mL)		
Median	1,600	
Range	18–423,350	

TACE transcatheter arterial chemoembolization, *PIVKAII* protein induced by vitamin K absence or antagonist-II

account of death due to hepatic failure (1 patient), variceal rupture (1 patient), or accidental perforation of the colon (1 patient)), and one patient remains alive without tumor progression. The median progression-free survival was 3.6 months. All patients were included in the survival assessment. Of the 25 patients, 21 died. The causes of death were tumor progression (18 patients), hepatic failure (1 patient), rupture of esophageal varices (1 patient), and accidental perforation of the colon (1 patient). The median survival time and 1-, 2-, and 3-year survival rates of the patients were 7.1 months and 36, 20, and 20 %, respectively (Fig. 1). The median survival time was 45.4 months in the patients who showed complete or partial response, and four of these patients survived for more than 3 years; on the other hand, the median survival time in the patients who showed stable or progressive disease was 5.8 months.

Adverse events

The adverse events occurring in the patients enrolled in this study are summarized in Table 2. The adverse events represent the maximum grade occurring in the patients during the entire course of therapy. Grade 3–4 leukocytopenia, neutropenia, and thrombocytopenia occurred in 5 (20 %), 2 (8 %), and 4 (16 %) of the patients, respectively; however, they were all transient and recovered fully without treatment. The major non-hematological adverse events were elevations of the serum AST and ALT levels. Grade 3–4 AST and ALT elevations were observed in 11 (44 %) and 6 (24 %) of the patients, respectively. However, the levels returned to the initial levels within one month without any additional treatment. No cumulative adverse events were seen in this patient series. One patient developed perforation of the colon on day 37 after the commencement of the first cycle; however, this was judged as an accidental event not causally related to the treatment. There were no other serious non-hematological adverse events.

Discussion

HAIC is widely undertaken in Japan for patients with advanced HCC who are not suitable candidates for

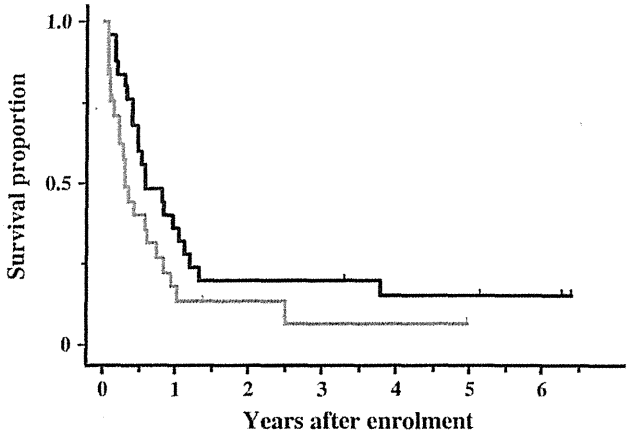

Fig. 1 Overall survival (*black line*) and progression-free survival (*gray line*) curves of the 25 patients of advanced hepatocellular carcinoma with tumor thrombosis in the main and/or first branch of the portal vein treated by hepatic arterial infusion chemotherapy using cisplatin. *Tick marks* indicate censored cases

Table 2 Adverse events

	Grade				
	1	2	3	4	3–4 (%)
Hemoglobin	6	7	0	0	0
Leukocytes	7	9	5	0	20
Neutrophils	6	7	2	0	8
Platelets	6	6	4	0	16
Nausea	10	5	0	0	0
Vomiting	9	1	0	0	0
Anorexia	13	6	0	0	0
Fatigue	8	3	0	0	0
Fever	3	0	0	0	0
Diarrhea	0	0	0	0	0
Abdominal pain	2	0	0	0	0
Weight loss	2	1	0	0	0
Total bilirubin	10	5	0	0	0
Hypoalbuminemia	6	7	0	0	0
AST	1	3	10	1	44
ALT	3	5	5	1	24
Alkaline phosphatase	3	0	0	0	0
Creatinine	3	2	0	0	0

AST, aspartate aminotransferase; ALT, alanine aminotransferase

resection, local ablative therapies, or transcatheter arterial chemoembolization, such as those with complicating PVTT [3, 4]. HAIC is usually administered using one of the following three well-reported regimens: cisplatin alone [11, 24], 5-FU plus cisplatin [12–15], and 5-FU plus interferon [16–20]. The efficacies of these regimens for HCC patients with PVTT are shown in Table 3 [11–20]. The reported response rates and disease control rates are approximately 20–40 % and 50–80 %, respectively, and the reported median survival is in the range of 7–12 months. However, optimum regimen for patients of advanced HCC with PVTT still remains controversial. Recently, a randomized phase II trial comparing 5-FU and interferon with best salvage therapy (BST), such as 5-FU plus cisplatin or cisplatin alone, has been reported [27]. Although the response rate was quite similar in both groups, the patients treated with 5-FU and interferon seemed to show inferior disease control and overall survival rates as compared to those treated by BST. Thus, the optimal regimen for HAIC has not yet been clarified. Transarterial radioembolization with yttrium-90 microspheres is one of the good options for HCC with PVTT, and the treatment efficacy has been reported to be favorable (Table 3) [28, 29]. However, this treatment has not been established as standard therapy, because the survival benefit has not been clarified by randomized trials.

In this study, cisplatin was selected as the trial chemotherapeutic agent for HAIC, because it is widely used in Japan, it can be administered by short infusion, and it requires no indwelling reservoir system for hepatic arterial infusion, unlike 5-FU plus cisplatin or 5-FU plus interferon. The response and disease control rates to HAIC with cisplatin in this study were 28 and 76 %, respectively, and the median overall survival time was 7.1 months. These results are comparable to previous reports (Table 3). Besides, in the patients who achieved complete or partial response, the median survival time was 45.4 months and four of them survived for more than 3 years. In previous reports also, the prognoses in the responders to HAIC were extremely favorable [11–13, 15–17, 19]. Thus, HAIC sometimes causes favorable tumor shrinkage, and a markedly prolonged survival time can be expected in such patients. If the tumor response to HAIC can be predicted prior to the start of the treatment, more appropriate selection of suitable candidates for HAIC may be possible. Therefore, identification of reliable markers to predict a favorable response to HAIC is warranted.

In comparison with systemic administration of anticancer agents, HAIC allows high local concentrations of anticancer drugs to be achieved, with reduced systemic distribution, thereby increasing the activity of the anticancer drug and reducing the likelihood of systemic adverse effects. With regard to the toxicity, the toxicity of HAIC with cisplatin was very mild. The main grade 3–4 adverse events were leukocytopenia (27 %), neutropenia (47 %), increased AST (40 %), and increased ALT (20 %). These adverse events were transient and reversed without any specific treatments. Furthermore, no cumulative or serious adverse events were seen in this study. Therefore, this treatment was considered to be well tolerated and even patients with Child-Pugh B could be included as candidates for this treatment.

HAIC is considered as one of the valid treatment options for advanced HCC, because it has been shown to exert a favorable effect with mild toxicities in advanced HCC patients with PVTT. However, it has not been acknowledged as a standard therapy for advanced HCC, because no chemotherapeutic agent or regimen has yet been shown to confer a survival benefit sufficient for adoption as a standard therapy [1–4]. On the other hand, sorafenib has been acknowledged as a standard agent for the treatment of patients with advanced HCC, including HCC with vascular invasion and extrahepatic metastases, because two pivotal phase III trials comparing sorafenib versus placebo have shown the survival benefit afforded by sorafenib [7, 8]. Sorafenib has a limited tumor shrinkage effect, but is capable of prolonging the time-to-progression and the overall survival. In the comparison of the efficacy between HAIC with cisplatin and sorafenib (Table 3), the efficacy of cisplatin seemed to be equivalent to that of sorafenib [7, 30]; therefore, cisplatin may be one of the promising

Table 3 Treatment efficacy of hepatic arterial infusion chemotherapy for hepatocellular carcinoma with portal vein tumor thrombosis

Regimen	*n*	RR (%)	DCR (%)	Median TTP/PFS (months)	Median OS (months)	1-year OS (%)	2-year OS (%)	3-year OS (%)	Median OS for responder (months)	References
Yttrium 90 (Child-Pugh A)	35	50	NA	5.6	10.4	NA	NA	NA	NA	Salem et al. [28]
Yttrium 90 (Child-Pugh B)	57	28	NA	5.9	5.6	NA	NA	NA	NA	Salem et al. [28]
Yttrium 90	76	NA	NA	NA	10.0	NA	NA	NA	NA	Sangro et al. [29]
Sorafenib[a]	108	NA	38.9	4.1	8.1	NA	NA	NA	NA	Bruix et al. [7]
Sorafenib[a]	44	NA	24	NA	4.4	NA	NA	NA	NA	Kang et al. [30]
5-FU/Cisplatin	48	48	77	NA	10.2	45.0	31.0	25.0	31.6	Ando et al. [12]
5-FU/Cisplatin	38	8	66	NA	6.0	21.0	NA	NA	NA	Cheong et al. [14]
5-FU/Cisplatin	18	33	72	NA	NA	28.0	NA	NA	15.0	Lai et al. [13]
5-FU/Cisplatin	52	39	65	4.1	15.9	53.3	34.8	26.1	40.7	Ueshima et al. [15]
5-FU/IFNα	55	44	51	5.2	11.8	48.9	28.6	16.4	24.4	Ota et al. [16]
5-FU/IFNα	116	52	54	NA	NA	34.0	18.0	NA	59 % (2 years)	Obi et al. [17]
5-FU/IFNα	31	29	55	5.8	7.5	29.0	5.6	NA	NA	Uka et al. [18]
5-FU/IFNα	102	39	47	2.0	9.0	36.8	21.2	10.8	25.0	Nagano et al. [19]
5-FU/IFNα	57	25	58	3.3	10.5	NA	NA	NA	NA	Yamashita et al. [20]
Cisplatin	24	21	25	NA	7.0	38.0	16.0	NA	37.3	Kondo et al. [11]
Current study (Cisplatin)	25	27	72	3.6	7.1	36	20	20	45.4	Ikeda

RR response rate, *DCR* disease control rate, *TTP* time to progression, *PFS* progression-free survival, *OS* overall survival, *5FU* 5-fluorouracil, *IFN* interferon, *NA* not available

[a] The study included the patients with macrovascular invasion

regimens for advanced HCC with PVTT. In addition, sorafenib and cisplatin have different toxicity profiles, except for causing liver dysfunction. Sorafenib and cisplatin have been reported to exert a synergistic effect against liver cancer in preclinical research [31, 32], and some clinical trials of combined regimens of sorafenib and cisplatin have been performed in patients with gastric cancer [33], nasopharyngeal carcinoma [34], and lung cancer [35]. Therefore, combined use of the two drugs may yield superior results. Furthermore, a randomized controlled trial comparing sorafenib plus HAIC with sorafenib could clarify the additional effect of HAIC and establish HAIC as a standard treatment for advanced HCC. Therefore, a phase I trial of sorafenib plus HAIC with cisplatin has already been conducted, and a randomized phase II trial of sorafenib plus HAIC with cisplatin versus sorafenib alone (UMIN000005703) is ongoing.

This study involved some limitations. First, the number of enrolled patients was not so high, and the results should be interpreted with some caution. Secondly, 10 patients received chemoembolization as prior therapy. This might lead to resistance to HAIC with cisplatin. Finally, as this was a single-arm phase II trial, the survival benefit of HAIC with cisplatin could not be clarified. All of these limitations argue for the conduct of a randomized trial to further compare this treatment with standard therapy in advanced HCC patients with PVTT.

In conclusion, HAIC with cisplatin exerts moderate activity with mild toxicity in HCC patients with PVTT. Especially, markedly prolonged survival can be expected in patients who respond to this treatment. At present, a randomized controlled trial of HAIC using a combination of cisplatin and sorafenib is under way.

Acknowledgments This work was supported in part by Grants-in-Aid for Cancer Research and for the Third-Term Comprehensive 10-Year Strategy for Cancer Control from the Ministry of Health, Labour, and Welfare of Japan and National Cancer Center Research and Development Fund (23-A-22).

Conflict of interest None.

References

1. El-Serag HB (2011) Hepatocellular carcinoma. N Engl J Med 365:1118–1127
2. Forner A, Llovet JM, Bruix J (2012) Hepatocellular carcinoma. Lancet 379:1245–1255
3. Kudo M, Izumi N, Kokudo N, Matsui O, Sakamoto M, Nakashima O, Kojiro M, Makuuchi M (2011) Management of hepatocellular carcinoma in Japan: consensus-Based Clinical Practice Guidelines proposed by the Japan Society of Hepatology (JSH) 2010 updated version. Dig Dis 29:339–364
4. Yamashita T, Kaneko S (2012) Treatment strategies for hepatocellular carcinoma in Japan. Hepatol Res. doi:10.1111/j.1872-034X.2012.01029.x

5. Llovet JM, Ricci S, Mazzaferro V, Hilgard P, Gane E, Blanc JF, de Oliveira AC, Santoro A, Raoul JL, Forner A, Schwartz M, Porta C, Zeuzem S, Bolondi L, Greten TF, Galle PR, Seitz JF, Borbath I, Häussinger D, Giannaris T, Shan M, Moscovici M, Voliotis D, Bruix J (2008) Sorafenib in advanced hepatocellular carcinoma. N Engl J Med 359:378–390
6. Cheng AL, Kang YK, Chen Z, Tsao CJ, Qin S, Kim JS, Luo R, Feng J, Ye S, Yang TS, Xu J, Sun Y, Liang H, Liu J, Wang J, Tak WY, Pan H, Burock K, Zou J, Voliotis D, Guan Z (2009) Efficacy and safety of sorafenib in patients in the Asia-Pacific region with advanced hepatocellular carcinoma: a phase III randomised, double-blind, placebo-controlled trial. Lancet Oncol 10:25–34
7. Bruix J, Raoul JL, Sherman M, Mazzaferro V, Bolondi L, Craxi A, Galle PR, Santoro A, Beaugrand M, Sangiovanni A, Porta C, Gerken G, Marrero JA, Nadel A, Shan M, Moscovici M, Voliotis D, Llovet JM (2012) Efficacy and safety of sorafenib in patients with advanced hepatocellular carcinoma: subanalyses of a phase III trial. J Hepatol 57:821–829
8. Cheng AL, Guan Z, Chen Z, Tsao CJ, Qin S, Kim JS, Yang TS, Tak WY, Pan H, Yu S, Xu J, Fang F, Zou J, Lentini G, Voliotis D, Kang YK (2012) Efficacy and safety of sorafenib in patients with advanced hepatocellular carcinoma according to baseline status: subset analyses of the phase III Sorafenib Asia-Pacific trial. Eur J Cancer 48:1452–1465
9. Ensminger WD, Gyves JW (1983) Regional chemotherapy of neoplastic diseases. Pharmacol Ther 21:277–293
10. Tzoracoleftherakis EE, Spiliotis JD, Kyriakopoulou T, Kakkos SK (1999) Intra-arterial versus systemic chemotherapy for non-operable hepatocellular carcinoma. Hepatogastroenterology 46:1122–1125
11. Kondo M, Morimoto M, Numata K, Nozaki A, Tanaka K (2011) Hepatic arterial infusion therapy with a fine powder formulation of cisplatin for advanced hepatocellular carcinoma with portal vein tumor thrombosis. Jpn J Clin Oncol 41:69–75
12. Ando E, Tanaka M, Yamashita F, Kuromatsu R, Yutani S, Fukumori K, Sumie S, Yano Y, Okuda K, Sata M (2002) Hepatic arterial infusion chemotherapy for advanced hepatocellular carcinoma with portal vein tumor thrombosis: analysis of 48 cases. Cancer 95:588–595
13. Lai YC, Shih CY, Jeng CM, Yang SS, Hu JT, Sung YC, Liu HT, Hou SM, Wu CH, Chen TK (2003) Hepatic arterial infusion chemotherapy for hepatocellular carcinoma with portal vein tumor thrombosis. World J Gastroenterol 9:2666–2670
14. Cheong JY, Lee KM, Cho SW, Won JH, Kim JK, Wang HJ, Hahm KB, Kim JH (2005) Survival benefits of intra-arterial infusion chemotherapy in patients with advanced hepatocellular carcinoma with portal vein tumor thrombosis. Hepatol Res 32:127–133
15. Ueshima K, Kudo M, Takita M, Nagai T, Tatsumi C, Ueda T, Kitai S, Ishikawa E, Yada N, Inoue T, Hagiwara S, Minami Y, Chung H (2010) Hepatic arterial infusion chemotherapy using low-dose 5-fluorouracil and cisplatin for advanced hepatocellular carcinoma. Oncology 78(Suppl 1):148–153
16. Ota H, Nagano H, Sakon M, Eguchi H, Kondo M, Yamamoto T, Nakamura M, Damdinsuren B, Wada H, Marubashi S, Miyamoto A, Dono K, Umeshita K, Nakamori S, Wakasa K, Monden M (2005) Treatment of hepatocellular carcinoma with major portal vein thrombosis by combined therapy with subcutaneous interferon-alpha and intra-arterial 5-fluorouracil; role of type 1 interferon receptor expression. Br J Cancer 93:557–564
17. Obi S, Yoshida H, Toune R, Unuma T, Kanda M, Sato S, Tateishi R, Teratani T, Shiina S, Omata M (2006) Combination therapy of intraarterial 5-fluorouracil and systemic interferon-alpha for advanced hepatocellular carcinoma with portal venous invasion. Cancer 106:1990–1997
18. Uka K, Aikata H, Takaki S, Miki D, Kawaoka T, Jeong SC, Takahashi S, Toyota N, Ito K, Chayama K (2007) Pretreatment predictor of response, time to progression, and survival to intra-arterial 5-fluorouracil/interferon combination therapy in patients with advanced hepatocellular carcinoma. J Gastroenterol 42:845–853
19. Nagano H, Wada H, Kobayashi S, Marubashi S, Eguchi H, Tanemura M, Tomimaru Y, Osuga K, Umeshita K, Doki Y, Mori M (2011) Long-term outcome of combined interferon-α and 5-fluorouracil treatment for advanced hepatocellular carcinoma with major portal vein thrombosis. Oncology 80:63–69
20. Yamashita T, Arai K, Sunagozaka H, Ueda T, Terashima T, Yamashita T, Mizukoshi E, Sakai A, Nakamoto Y, Honda M, Kaneko S (2011) Randomized, phase II study comparing interferon combined with hepatic arterial infusion of fluorouracil plus cisplatin and fluorouracil alone in patients with advanced hepatocellular carcinoma. Oncology 81:281–290
21. Groupe d'Etude et de Traitement du Carcinome Hepatocellulaire (1995) A comparison of lipiodol chemoembolization and conservative treatment for unresectable hepatocellular carcinoma. N Engl J Med 332:1294–1296
22. Pelletier G, Ducreux M, Gay F, Luboinski M, Hagège H, Dao T, Van Steenbergen W, Buffet C, Rougier P, Adler M, Pignon JP, Roche A (1998) Treatment of unresectable hepatocellular carcinoma with lipiodol chemoembolization: a multicenter randomized trial. J Hepatol 29:129–134
23. Lo CM, Ngan H, Tso WK, Liu CL, Lam CM, Poon RT, Fan ST, Wong J (2002) Randomized controlled trial of transarterial lipiodol chemoembolization for unresectable hepatocellular carcinoma. Hepatology 35:1164–1171
24. Yoshikawa M, Ono N, Yodono H, Ichida T, Nakamura H (2008) Phase II study of hepatic arterial infusion of a fine-powder formulation of cisplatin for advanced hepatocellular carcinoma. Hepatol Res 38:474–483
25. World Health Organization (1979) WHO handbook for reporting results of cancer treatment, vol 48. World Health Organization, Geneva
26. Simon R (1987) How large should a phase II trial of a new drug be? Cancer Treat Rep 71:1079–1085
27. Monden M, Sakon M, Sakata Y, Ueda Y, Hashimura E, FAIT Research Group (2012) 5-fluorouracil arterial infusion + interferon therapy for highly advanced hepatocellular carcinoma: a multicenter, randomized, phase II study. Hepatol Res 42:150–165
28. Salem R, Lewandowski RJ, Mulcahy MF, Riaz A, Ryu RK, Ibrahim S, Atassi B, Baker T, Gates V, Miller FH, Sato KT, Wang E, Gupta R, Benson AB, Newman SB, Omary RA, Abecassis M, Kulik L (2010) Radioembolization for hepatocellular carcinoma using Yttrium-90 microspheres: a comprehensive report of long-term outcomes. Gastroenterology 138:52–64
29. Sangro B, Carpanese L, Cianni R, Golfieri R, Gasparini D, Ezziddin S, Paprottka PM, Fiore F, Van Buskirk M, Bilbao JI, Ettorre GM, Salvatori R, Giampalma E, Geatti O, Wilhelm K, Hoffmann RT, Izzo F, Iñarrairaegui M, Maini CL, Urigo C, Cappelli A, Vit A, Ahmadzadehfar H, Jakobs TF, Lastoria S, European Network on Radioembolization with Yttrium-90 Resin Microspheres (ENRY) (2011) Survival after yttrium-90 resin microsphere radioembolization of hepatocellular carcinoma across Barcelona clinic liver cancer stages: a European evaluation. Hepatology 54:868–878
30. Kang YK, Guan Z, Chen Z, Tsao CJ, Qin S, Kim JS, Burock K, Zou J, Voliotis D, Cheng AL (2008) Sorafenib is effective in patients from the Asia-Pacific region with hepatocellular carcinoma (HCC): subgroup analysis of effect of macroscopic vascular invasion, extrahepatic spread, and ECOG performance status on outcome. Hepatology 48(suppl 1):976A (abstr 1505)

31. Chen FS, Cui YZ, Luo RC, Wu J, Zhang H (2008) Coadministration of sorafenib and cisplatin inhibits proliferation of hepatocellular carcinoma HepG2 cells in vitro. Nan Fang Yi Ke Da Xue Xue Bao 28:1684–1687
32. Eicher C, Dewerth A, Thomale J, Ellerkamp V, Hildenbrand S, Warmann SW, Fuchs J, Armeanu-Ebinger S (2013) Effect of sorafenib combined with cytostatic agents on hepatoblastoma cell lines and xenografts. Br J Cancer 108:334–341
33. Sun W, Powell M, O'Dwyer PJ, Catalano P, Ansari RH, Benson AB 3rd (2010) Phase II study of sorafenib in combination with docetaxel and cisplatin in the treatment of metastatic or advanced gastric and gastroesophageal junction adenocarcinoma: ECOG 5203. J Clin Oncol 28:2947–2951
34. Xue C, Huang Y, Huang PY, Yu QT, Pan JJ, Liu LZ, Song XQ, Lin SJ, Wu JX, Zhang JW, Zhao HY, Xu F, Liu JL, Hu ZH, Zhao LP, Zhao YY, Wu X, Zhang J, Ma YX, Zhang L (2013) Phase II study of sorafenib in combination with cisplatin and 5-fluorouracil to treat recurrent or metastatic nasopharyngeal carcinoma. Ann Oncol 24:1055–1061
35. Paz-Ares LG, Biesma B, Heigener D, von Pawel J, Eisen T, Bennouna J, Zhang L, Liao M, Sun Y, Gans S, Syrigos K, Le Marie E, Gottfried M, Vansteenkiste J, Alberola V, Strauss UP, Montegriffo E, Ong TJ, Santoro A, NSCLC [non-small-cell lung cancer] Research Experience Utilizing Sorafenib (NExUS) Investigators Study Group (2012) Phase III, randomized, double-blind, placebo-controlled trial of gemcitabine/cisplatin alone or with sorafenib for the first-line treatment of advanced, nonsquamous non-small-cell lung cancer. J Clin Oncol 30:3084–3092

J Gastroenterol
DOI 10.1007/s00535-013-0853-7

ORIGINAL ARTICLE—LIVER, PANCREAS, AND BILIARY TRACT

Efficacy of sorafenib in patients with hepatocellular carcinoma refractory to transcatheter arterial chemoembolization

Masafumi Ikeda · Shuichi Mitsunaga · Satoshi Shimizu · Izumi Ohno · Hideaki Takahashi · Hiroyuki Okuyama · Akiko Kuwahara · Shunsuke Kondo · Chigusa Morizane · Hideki Ueno · Mitsuo Satake · Yasuaki Arai · Takuji Okusaka

Received: 5 March 2013 / Accepted: 9 June 2013

Abstract
Background The efficacy of sorafenib for hepatocellular carcinoma (HCC) patients refractory to transcatheter arterial chemoembolization (TACE) has not yet been clarified. We investigated the efficacy of sorafenib in HCC patients who were refractory to TACE (sorafenib group) and retrospectively compared the results with those of patients treated with hepatic arterial infusion chemotherapy using cisplatin (cisplatin group).
Methods We evaluated the anti-tumor effect, the time to progression, and the overall survival in 48 patients in the sorafenib group and 66 patients in the cisplatin group.
Results The disease control rate to sorafenib was 60.4 %, the median time to progression was 3.9 months, and the median survival time was 16.4 months in patients who were refractory to TACE. When compared with the cisplatin group, significant differences in the patient characteristics were not observed between the two groups with the exception of patient age; however, the disease control rate (cisplatin group 28.8 %, $P = 0.001$), time to progression (cisplatin group: median 2.0 months, hazard ratio 0.44, $P < 0.01$), and overall survival (cisplatin group: median 8.6 months, hazard ratio 0.57, $P < 0.001$) were significantly superior in the sorafenib group. The multivariate analysis also showed the sorafenib treatment to be the most significant factor contributing to prolongation of time to progression and overall survival.
Conclusions Sorafenib showed favorable treatment results in patients refractory to TACE. When compared with hepatic arterial infusion chemotherapy using cisplatin, sorafenib demonstrated a significantly higher disease control rate, a longer time to progression and increased overall survival.

Keywords Hepatocellular carcinoma · Sorafenib · Cisplatin · Chemotherapy · Hepatic arterial infusion chemotherapy

Introduction

Hepatocellular carcinoma (HCC) is one of the most common malignancies worldwide. HCC is highly prevalent in African and Asian countries, and its incidence has recently been increasing in western countries [1, 2]. For patients with unresectable HCC who are not candidates for curative treatments, such as resection, transplantation, or local ablation, transcatheter arterial chemoembolization (TACE) is the main therapeutic option [1, 2]. A clear survival benefit for patients with unresectable HCC who are treated with TACE has been shown in several randomized controlled trials and a meta-analysis [3, 4]. Chemotherapy has been recognized as a palliative treatment option for patients with highly advanced HCC in whom TACE is not indicated.

Sorafenib is a multikinase inhibitor of Raf kinase, which is involved in cancer cell proliferation, as well as vascular

M. Ikeda (✉) · S. Mitsunaga · S. Shimizu · I. Ohno · H. Takahashi · H. Okuyama · A. Kuwahara
Division of Hepatobiliary and Pancreatic Oncology, National Cancer Center Hospital East, 6-5-1 Kashiwanoha, Kashiwa, Chiba 277-8577, Japan
e-mail: masikeda@east.ncc.go.jp

S. Kondo · C. Morizane · H. Ueno · T. Okusaka
Hepatobiliary and Pancreatic Oncology Division, National Cancer Center Hospital, Tokyo, Japan

M. Satake
Division of Diagnostic Radiology, National Cancer Center Hospital East, Kashiwa, Japan

Y. Arai
Department of Diagnostic Radiology, National Cancer Center Hospital, Tokyo, Japan

Published online: 23 June 2013

endothelial growth factor receptor-2/-3 (VEGFR-2/-3) and platelet-derived growth factor receptor beta (PDGFR-β), which is involved in peritumor neovascularization [5, 6]. In two pivotal international phase 3 trials of sorafenib vs. placebo, the so-called SHARP trial [7] and the Asia-Pacific trial [8], sorafenib demonstrated a prolonged overall survival and time-to-progression, compared with a placebo, in patients with advanced hepatocellular carcinoma (HCC). Therefore, sorafenib has been acknowledged as a standard therapy for advanced HCC.

In the therapeutic strategy of the Barcelona Clinic Liver Cancer Study Group [5], sorafenib was indicated for patients with extrahepatic metastasis and/or vascular invasion of Stage C disease (advanced stage), patients with a performance status (PS) of 1–2, and those with Stage B (intermediate stage) multifocal HCC refractory to TACE. In the 2010 updated version of the consensus-based clinical practice guidelines for the management of HCC proposed by the Japan Society of Hepatology [9, 10], patients with extrahepatic metastasis, with macrovascular invasion, and who were refractory to TACE are listed in the algorithm for treatment with sorafenib. The main indications for sorafenib are, therefore, considered to be patients who are refractory to TACE, those who have vascular invasion, or those who have extrahepatic metastasis. Subgroup analyses of the SHARP trial [7] and the Asia-Pacific trial [8] showed the treatment efficacies in patients with vascular invasion and extrahepatic metastasis. However, those in patients who are refractory to TACE have not been reported so far, although the outcome of patients with prior TACE has been reported [11, 12].

Before the introduction of sorafenib, hepatic arterial infusion chemotherapy was mainly performed in Japan for patients with advanced HCC [13–21], including those refractory to TACE [13, 14]. However, no consensus on a standard therapy has been achieved because large-scale prospective studies and randomized controlled studies have not been conducted and the survival benefit has not been clarified [10]. In this study, we clarified the efficacy of sorafenib in patients who were refractory to TACE (sorafenib group) and retrospectively compared the anti-tumor effect, time to progression, and overall survival between the sorafenib group and patients who were refractory to TACE and who were treated with hepatic arterial infusion chemotherapy using cisplatin (cisplatin group).

Patients and methods

Patients

Forty-eight consecutive chemotherapy-naive patients who were refractory to TACE without extrahepatic metastasis were extracted from 205 patients treated with sorafenib at the National Cancer Center Hospital East (East Hospital) between April 2009 and December 2011. Sixty-six of the 84 chemo-naive patients who were refractory to TACE and were treated with hepatic arterial infusion chemotherapy using cisplatin at the National Cancer Center Hospital and the East Hospital between July 2004 and September 2008, the period before the approval of sorafenib in Japan, were enrolled in the cisplatin group after excluding 18 patients with extrahepatic metastasis or the moderate retention of ascites. In this series, the total number of TACE sessions was 478, while the median number of TACE sessions was 4 (range 1–16). In previous TACE sessions, an emulsion containing an anticancer agent and lipiodol followed by gelatin sponge particles were used. In the present series, epirubicin was used for 394 sessions, adriamycin was used for 29 sessions, and mitomycin C was used for 12 sessions; the anticancer agent was unknown for 43 sessions. Patients who were refractory to TACE were defined as those showing progression or a tumor shrinkage rate of <25 % of the hypervascular lesions as visualized using dynamic computed tomography (CT) and/or magnetic resonance imaging (MRI) after 1–3 months of TACE [13]. The TACE-refractory status of individual patients was discussed at a weekly tumor board conference. HCC was diagnosed based on the presence of histopathological findings or imaging findings that were characteristic of HCC together with an increase in the serum α-fetoprotein level. The diameter of the tumor and the presence/absence of extrahepatic metastasis were confirmed using dynamic CT/MRI, ultrasound, or chest X-ray/CT prior to treatment. In our hospital, sorafenib is indicated for the treatment of patients with highly advanced HCC with a Child–Pugh score of either A or B. Informed consent for each treatment was obtained from all the patients before the initiation of treatment. This clinical study was conducted with the approval of the Ethics Committee of the National Cancer Center and was conducted in accordance with the ethical principals stated in the Japanese ethics guideline for epidemiological research.

Treatments

An oral dose of sorafenib at 400 mg was administered twice daily, after breakfast and dinner (800 mg/day). Treatment was continued as long as tolerability was observed without obvious disease progression. The dose was reduced or withdrawn and treatment was continued depending on the severity of adverse events. A dose increase up to 800 mg/day was permitted when the dose increase was judged possible in patients in whom the dose had been reduced.

For hepatic arterial infusion chemotherapy using cisplatin, intra-arterial cisplatin at a dose of 65 mg/m^2 was

administered over 20–40 min via a catheter inserted into the feeding arteries of the tumors. Treatment was repeated every 4–6 weeks for up to 6 courses until disease progression or unacceptable toxicities occurred. An infusion of 3,000 mL or more was administered on the day of treatment, and an infusion of 1,000 mL or more was continued for 3 days after administration to reduce renal toxicity caused by cisplatin; a diuretic (mannitol, furosemide, etc.) was administered as necessary to ensure an adequate urine volume.

Assessment and statistical analyses

Dynamic CT or MRI was used to confirm the anti-tumor effect every 1–2 months. The anti-tumor effect was evaluated using the Response Evaluation Criteria in Solid Tumors, version 1.0 (RECIST) [22], to judge the best overall response. The time to progression was defined as the period from the date of the start of treatment until the date of the confirmation of tumor progression by radiological evaluation or the day on which obvious tumor progression was judged to have occurred based on the clinical symptoms. Overall survival was defined as the period from the day of the start of treatment until the date of death or the final date of confirmed survival. A χ^2 test or Wilcoxon test was used to compare the patient characteristics and the anti-tumor effect between the sorafenib and the hepatic arterial infusion chemotherapy using cisplatin groups, and the Kaplan–Meier method was used to calculate the time to progression and the overall survival; the log-rank test was used to analyze differences between the groups. In a multivariate analysis, a Cox regression was used to analyze factors with $P < 0.10$ using a univariate analysis. $P < 0.05$ was judged to be statistically significant. JMP version 9.0 (SAS Institute Inc.) was used for the above statistical analyses.

Results

Patient characteristics

Table 1 shows the patient characteristics before each treatment. Age was significantly higher in the sorafenib group, although the medians were very similar (sorafenib group 71 years, cisplatin group 69 years). Although the Eastern Cooperative Oncology Group PS, the maximum tumor diameter, total bilirubin, AST, and ALT tended to be slightly worse in the cisplatin group, significant differences were not observed in the other parameters between the two groups. The median number of treatments in the cisplatin group was 2 (range 1–6 times). As a subsequent treatment, other systemic chemotherapy was performed in 14 patients, hepatic arterial infusion chemotherapy using cisplatin was performed in 7 patients, TACE was performed in 4 patients, and hepatic arterial infusion chemotherapy using 5-FU + interferon and radiotherapy was performed in one patient each in the sorafenib group; meanwhile, TACE was performed in 15 patients, hepatic arterial infusion chemotherapy using epirubicin was performed in 4 patients, other systemic chemotherapy was performed in 4 patients, hepatic arterial infusion chemotherapy using 5-FU + interferon was performed in 2 patients, and radiotherapy was performed in one patient in the cisplatin group. The median observation period was 9.4 months (range 2.1–31.6 months) in the sorafenib group and 7.5 months (range 0.8–43.1 months) in the cisplatin group; this difference was not statistically significant ($P = 0.44$).

Efficacy

The best overall response in the sorafenib group was evaluated as a complete response (CR) in one patient, a partial response (PR) in 2 patients, stable disease (SD) in 26 patients, progressive disease (PD) in 16 patients, and not evaluable (NE) in 3 patients. The response rate (CR + PR) was 6.3 % [95 % confidence interval (CI) 1.3–17.2 %], and the disease control rate (CD + PR + SD) was 60.4 % (95 % CI 45.3–74.2 %). The median time to progression and the progression-free rate at 6- and 12-months were 3.9 months, 32.6 %, and 12.1 %, respectively, while the median overall survival and the survival rate at 6-, 12-, and 24-months was 16.4 months, 88.9 %, 55.3 %, and 32.5 %, respectively, in the sorafenib group.

The best overall response in the cisplatin group was evaluated as a CR in 1 patient, PR in 0 patients, SD in 18 patients, PD in 39 patients, and NE in 8 patients. The response rate was 1.5 % (95 % CI 0.04–8.2 %), and a significant difference in the response rate, compared with the sorafenib group, was not observed ($P = 0.40$). The disease control rate was 28.8 % (95 % CI 18.3–41.3 %), which was significantly higher in the sorafenib group ($P = 0.001$). The median time to progression and the progression-free rate at 6- and 12-months in the cisplatin group was 2.0 months, 15.9 %, and 4.8 %, respectively, showing a significantly superior result in the sorafenib group (hazard ratio 0.44, $P < 0.01$) (Fig. 1). At the time of analysis, 21 patients had died because of tumor progression, and 1 patient had died because of hepatic failure in the sorafenib group. Additionally, 60 patients had died because of tumor progression, and 4 patients had died because of hepatic failure in the cisplatin group. The median survival time and the survival rate at 6-, 12-, and 24-months in the cisplatin group were 8.6 months, 62.0 %, 35.2 %, and 11.3 %, respectively, showing a significantly superior result in the sorafenib group (hazard ratio: 0.57,

Table 1 Patient characteristics

	Sorafenib		Cisplatin		*P* value
	n	(%)	*n*	(%)	
All patients	48	–	66	–	
Age (years)					
Median [range]	71	[53–83]	69	[40–82]	0.04
Sex					
Male	43	(90)	52	(79)	
Female	5	(10)	14	(21)	1.00
Performance status					
0	43	(90)	49	(74)	
1	5	(10)	17	(26)	0.07
HCVAb (positive)	32	(67)	45	(68)	1.00
HBsAg (positive)	7	(15)	8	(12)	0.92
Prior resection (present)	12	(25)	27	(41)	0.11
Prior ablation (present)	19	(40)	29	(44)	1.00
No. of prior TACE sessions					
Median [range]	4	[1–9]	4	[1–17]	0.86
Maximum tumor diameter (mm)					
Median [range]	30.5	[10–150]	40	[12–110]	0.07
Number of tumors					
1–3	8	(17)	13	(20)	0.32
≥4	40	(83)	53	(80)	0.64
Portal vein invasion (present)	9	(19)	16	(24)	0.64
Hepatic vein invasion (present)	3	(6)	4	(6)	0.99
Stage[a]					
II or III	38	(79)	49	(74)	
IVa	10	(21)	17	(26)	0.70
Ascites (present)	9	(19)	17	(26)	0.51
Child–Pugh class					
A	32	(67)	36	(55)	
B	16	(33)	30	(45)	0.27
Total bilirubin (mg/dL)					
Median [range]	0.9	[0.3–2.1]	1.1	[0.2–3.0]	0.02
Albumin (g/dL)					
Median [range]	3.5	[2.3–4.8]	3.3	[2.4–4.5]	0.21
AST (U/L)					
Median [range]	54	[20–165]	88	[35–287]	0.04
ALT (U/L)					
Median [range]	43	[10–139]	62	[22–187]	0.05
Prothrombin time (%)					
Median [range]	78	[40–107]	73	[48–104]	0.39
α-Fetoprotein (ng/mL)					
Median [range]	70.3	[1.3–218876]	324.3	[1.7–210200]	0.59
PIVKAII (mAU/mL)					
Median [range]	505.5	[11–291330]	438	[11–96390]	0.65
Subsequent treatments (present)	27	(56)	26	(39)	0.11

HCVAb hepatitis C viral antibody, *HBsAg* hepatitis B surface antigen, *TACE* transcatheter arterial chemoembolization, *AST* aspartate aminotransferase, *ALT* alanine aminotransferase, *PIVKAII* protein induced by vitamin K absence or antagonists-II

[a] Japanese classification of primary liver cancer